IEEE Access
Multidisciplinary ⋮ Rapid Review ⋮ Open Access Journal

Received 30 April 2026, accepted 13 May 2026, date of publication 18 May 2026, date of current version 21 May 2026.

Digital Object Identifier 10.1109/ACCESS.2026.3694117

RESEARCH ARTICLE

Experimental Validation of 5G Positioning With Inter-Cell Clock Bias Correction

PENGHUI XU[1], (Member, IEEE), MATTIA BRAMBILLA[2], (Senior Member, IEEE), BERNARDO CAMAJORI TEDESCHINI[2], (Member, IEEE), AND MONICA NICOLI[3], (Senior Member, IEEE)

[1]Department of Aeronautical and Aviation Engineering, The Hong Kong Polytechnic University, Hong Kong
[2]Department of Electronics, Information and Bioengineering, Politecnico di Milano, 20133 Milan, Italy
[3]Department of Management, Economics and Industrial Engineering, Politecnico di Milano, 20133 Milan, Italy

Corresponding author: Mattia Brambilla (mattia.brambilla@polimi.it)

ABSTRACT The advancement of fifth generation (5G) cellular networks offers significant opportunities for positioning services, yet the performance of these systems is currently hindered by the clock offset among 5G base stations in commercial networks, here referred to as inter-cell clock bias (ICCB). These biases introduce systematic errors in time of arrival (TOA) measurements, degrading localization accuracy. This paper addresses this challenge by utilizing a stationary reference receiver to estimate and correct the ICCBs. By aligning the timing references of multiple base stations, our single-difference correction method enables accurate standalone positioning using opportunistically received synchronization signal block (SSB) data. The proposed method was validated with three independent measurement campaigns at the same rural location on broadcast signals from a commercial 5G network. The results demonstrate the effectiveness of the ICCB correction, showing a 73%-84% reduction in positioning error compared to uncompensated methods. Applying a smoothing filter to the ICCB corrections further improves the mean accuracy by about 18%-19%, achieving a mean error between 12.7m and 20.6m across the three tests. While this performance is constrained by the limited bandwidth of the current commercial 5G deployment at 3.68 GHz, our findings confirm the feasibility of leveraging public 5G signals for location-based services.

INDEX TERMS 5G mobile communication, cellular networks, clock bias, location-based services, positioning.

I. INTRODUCTION

The evolution of fifth generation (5G) cellular networks has unlocked new opportunities for positioning, complementing traditional global navigation satellite systems (GNSS) and giving rise to heterogeneous systems for localization and navigation [1], [2], [3], [4]. The latest releases of the cellular communication standard have introduced enhanced positioning functionalities to address the needs of connected automated driving and industrial Internet of things (IIoT) use cases [5], [6]. From the specification of dedicated cellular positioning signals in the 3rd Generation Partnership Project (3GPP) Release 16 [7], [8], up to the recent standardization of bandwidth aggregation and carrier phase positioning in 3GPP Release 18 [9], 5G positioning emerges as a key asset and facility for technologically-advanced industries [10].

While the roadmap for 5G positioning standardization is defined, currently available network deployments still face a low level of technological maturity and readiness, leaving the assessment of commercial 5G positioning potentials to a few research studies. Simulations offer valuable insights into performance bounds and parameter sensitivity [11], [12], [13], [14], [15], [16], [17], yet real-world signals are necessary to validate the effectiveness of a cellular positioning service. To this end, approaches based on opportunistic signal decoding from the public network [1], [18], [19], [20], [21], [22], [23], [24], [25], [26] or the emulation through software-defined radio (SDR) testbeds [27], [28], [29], [30], [31], [32], [33], [34] have been adopted by researchers. Complementary experimental measurement campaigns have

The associate editor coordinating the review of this manuscript and approving it for publication was Abbas Kiani.

also been conducted in adjacent low-power IoT cellular technologies, such as NB-IoT path-loss characterization in urban outdoor environments [35], providing empirical context on commercial cellular signal propagation. Simulated use cases are especially suitable for assessing the potential performances at millimeter wave (mmWave) [36], [37], where the hardware availability and its ease of use is a challenge.

An SDR implementation of a local private network offers the possibility of transmitting and receiving dedicated positioning signals that are currently not implemented in commercial networks, such as the positioning reference signal (PRS) or the sounding reference signal (SRS), in compliance with the 3GPP technical specifications [8]. While such signals are not yet available for public users in real network deployments, literature works have shown that it is possible to opportunistically detect synchronization signals periodically broadcasted by cellular base stations (BSs) (i.e., gNodeBs (gNBs)) for cell discovery purposes. This is exactly the approach pursued in this work, where we target the positioning of a user equipment (UE) through time of arrival (TOA) measurements from multiple gNBs.

A primary obstacle arising when using signals from multiple gNBs is the lack of precise synchronization. This results in a significant clock offset between the gNBs, which is referred to as inter-cell clock bias (ICCB), introducing systematic errors into time-based measurements like TOA and degrading the positioning accuracy. Indeed, experimental analysis by Barbieri et al. [38] on operational 5G networks has highlighted that current network synchronization instabilities can lead to ranging errors in the order of ± 60 m or more, resulting from TOA fluctuations exceeding ± 200 ns in rural environments.

To address this specific issue, the literature has explored advanced positioning techniques along with joint synchronization and localization methodologies. The experimental study in [19] was carried out by placing a network scanner in several known locations, and computing receiver clock bias based on the actual distance and the measured TOA. Such compensation could significantly improve the positioning accuracy, yet it is almost impossible to obtain in real practice. The comprehensive carrier phase positioning (CPP) technique proposed in Fan et al. [39] achieves precise clock synchronization among base stations, though it relies on the gNBs being able to measure signals from each other, which is not always feasible in commercial deployments. The work by Chen et al. [30] cleverly circumvents the issue of ICCB by conducting experiments with only a single gNB, a scenario that is unfortunately not scalable for general wide-area positioning. A more practical approach for commercial networks involves employing a stationary reference receiver, a concept borrowed from high-precision GNSS. For example, Fouda et al. [40] utilize a classic double-difference (DD) method to cancel clock errors. However, this approach has practical drawbacks, as it inherently amplifies measurement noise variance.

This paper presents a framework that relies on a reference receiver to address the above-mentioned limitations through a single-difference (SD)-based correction method. Our approach exploits the stationary receiver to first estimate the raw clock biases existing between gNBs via SD operation. We then apply a smoothing filter to this data stream to generate a clean, low-noise correction signal. This correction is then applied directly to the TOA measurements. By pre-filtering noisy ranging measurements and then applying the correction, our method improves positioning robustness under real-world conditions. This allows us to leverage existing commercial 5G signals for positioning without the need for a fully synchronized network. To summarize, our key contributions are as follows:

- A systematic analysis of single-difference ICCB correction for synchronization signal block (SSB)-TOA positioning, demonstrating that the SD formulation avoids the noise amplification inherent in DD methods, which is particularly detrimental under the high-noise conditions of opportunistic SSB measurements in commercial networks;
- An investigation of the temporal characteristics of the ICCB and a noise mitigation strategy based on moving average smoothing applied directly to the raw SD ICCB estimates, suppressing measurement noise prior to the positioning solution;
- Empirical validation of the proposed framework using measurements from an operational commercial 5G network, providing experimental evidence that bridges the gap between the theoretical ICCB characterization in the literature and its practical correction for positioning.

In the remainder of the paper, Section II focuses on the related work; Section III presents the methodology for the 5G SSB-based opportunistic positioning algorithm using ICCB; Section IV reports the results obtained with real measurements; Section V is the conclusion and outlines directions for future work.

II. RELATED WORK

A main novelty for positioning foreseen by the forthcoming cellular network is the introduction of advanced localization algorithms that enhance the accuracy of solutions employing traditional measurements. In this regard, the concept of CPP [30], [39] has been introduced in 3GPP Release 18 [41], [42], and researchers have benchmarked the performance through simulations [39] or even through data collection with an SDR measuring SSB from a single indoor BS [30]. The carrier-phase positioning algorithm for systems without synchronization (CPASS), proposed in both batch and sequential real-time versions, was proven to enable the estimation of the UE position overcoming the need for BS synchronization [43]. In that work, authors perform field experiments but not adhering to the 5G protocol. The CPASS introduces a static reference station as a clock bias monitoring (CBM) station and uses double-difference to eliminate clock biases, requiring the presence of an additional network

apparatus for positioning. A cooperative version of the CPP has been presented as well [44], where the asynchronous devices can be both static and mobile.

To offer cm-level positioning accuracy, all the above discussed methods also call for a dedicated network unit (preferably static) in charge of simultaneously measuring the signals with a UE from multiple BSs and use them for compensating the error introduced by the clock biases. The external unit (i.e., the CBM in [43]), which is referred as positioning reference unit (PRU) by 3GPP [45] has the main functionality of removing the clock bias terms of the BSs. To this goal, the PRU must be preferably fixed and strategically placed in a known location, possibly with good visibility to guarantee the signal reception from multiple BSs. The PRU can assist the UE by providing the required information for UE-based positioning, or report measurements to a location measurement function (LMF) embedded in the cellular network for UE-assisted LMF-based positioning. Practically, in the perspective of a positioning service, the role of the PRU is to provide sufficient correction terms for improved positioning. From a network perspective, it can be assimilated to a static UE. According to the PRU availability, as well as on other contextual information on the number of available BSs and their signal quality, the LMF of the cellular network can choose the positioning algorithm to be used.

This paper builds upon the PRU concept but diverges from traditional CPP in two fundamental ways. First, whereas CPP methods often assume the availability of dedicated carrier phase reference signals, our framework is designed to work with the opportunistically received SSB, a signal that is broadcast by all commercial 5G base stations for cell discovery. This makes our approach more practical for immediate use in existing network deployments where dedicated positioning signals may not be active.

Second, our method differs algorithmically from the DD technique common in CPP and CPASS. We propose an SD correction framework where the PRU first estimates the raw ICCBs and, crucially, applies a smoothing filter to generate a high-quality, low-noise correction signal. This correction is then applied directly to the UE TOA measurements. This SD architecture avoids the noise amplification inherent in DD and eliminates the strict common view requirement, offering a more robust and practical solution for positioning within today's commercial 5G networks.

III. 5G POSITIONING WITH ICCB CORRECTION METHODOLOGY

The proposed localization system model is illustrated in Fig. 1. It consists of 5G gNBs, a stationary PRU at a known location, and a UE whose position is to be determined. The PRU estimates the relative clock biases, referred to as ICCB, between a reference BS and all other BSs. The UE then uses these ICCB values to correct its raw TOA measurements before solving its navigation equations, mitigating the error introduced by inaccurate BS synchronization.

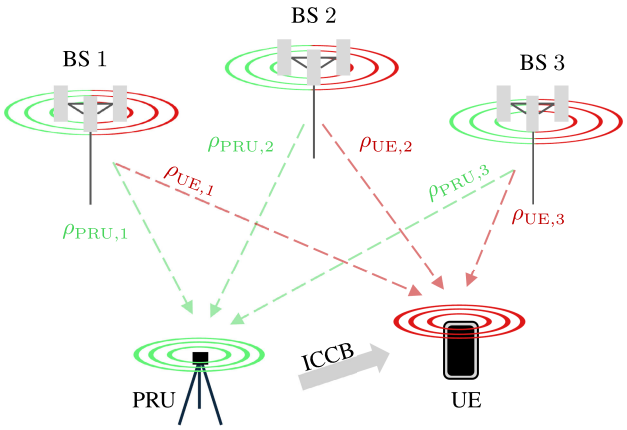

FIGURE 1. Illustration of the considered 5G positioning system comprising BSs, a PRU for ICCB broadcasting, and a UE.

In the following, we first formulate the mathematical model for TOA measurements and the associated rank deficiency problem. Then, we detail the single-difference approach to estimate the raw ICCB at the PRU and the smoothing filter applied for noise mitigation. Finally, we derive the corrected ranging equation that allows the UE to perform standalone positioning.

A. TOA MEASUREMENT MODEL

The 5G TOA measurement is drawn by the UE using the downlink signal received from the BS i, and it is expressed as:

$$\begin{aligned}\rho_{\mathrm{UE},i} &= R_{\mathrm{UE},i} + c(\Delta t_{\mathrm{UE}} - \Delta t_i) + \eta_{\mathrm{UE},i} \\ &= R_{\mathrm{UE},i} + \delta_{\mathrm{UE}} - \delta_i + \eta_{\mathrm{UE},i} \\ &= R_{\mathrm{UE},i} + \delta_{\mathrm{UE},i} + \eta_{\mathrm{UE},i},\end{aligned} \tag{1}$$

where $R_{\mathrm{UE},i}$ represents the geometrical distance between the UE and BS i, Δt_{UE} is the receiver clock bias, while Δt_i is the clock bias of the i-th BS, with both biases referred to a common timing system (e.g., the UTC time). c is the speed of light. For simplicity, the clock bias in the unit of second is converted to meters, represented as $\delta_{\mathrm{UE},i} = \delta_{\mathrm{UE}} - \delta_i = c\,(\Delta t_{\mathrm{UE}} - \Delta t_i)$. $\eta_{\mathrm{UE},i}$ represents the measurement uncertainty accounting for background noise and interference at the receiver, along with multipath and propagation conditions. It is noted that antenna-dependent effects, such as group-delay and phase pattern variations, are also implicitly included in this term. Since these effects depend on the angle of arrival, the effective TOA may vary for different signal directions, which implies that the PRU-derived correction is most accurate when the PRU and UE observe the BSs from similar angles.

The ICCB arises due to clock offsets among time references at different 5G BSs. Since TOA-based positioning assumes precise timing, any bias in the time source leads to positioning biases. Assuming N TOA measurements are available, the UE state for positioning includes $\mathbf{p}_{\mathrm{UE}} = [x_{\mathrm{UE}}\ y_{\mathrm{UE}}\ z_{\mathrm{UE}}]^\top$ and different clock biases $[\delta_1\ \delta_2\ \cdots\ \delta_N]^\top$, totally $(3+N)$ states. The rank deficiency in the design matrix prevents standalone positioning from being achieved solely

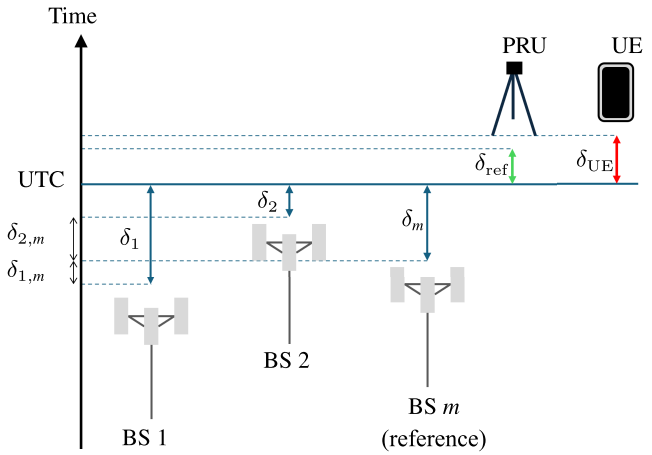

FIGURE 2. Illustration of ICCB $\delta_{i,m}$, clock bias of the UE δ_{UE}, PRU δ_{ref} and the BSs δ_i.

through the snapshot TOAs using least squares estimation methods.

B. ICCB ESTIMATION VIA SINGLE-DIFFERENCE

To reduce the number of states to be estimated, ICCB compensation is introduced. Assuming a 5G receiver at a known position $\mathbf{p}_{\text{ref}} = [x_{\text{ref}}\, y_{\text{ref}}\, z_{\text{ref}}]^\top$, which can be identified in the PRU, and measuring the TOAs from multiple BSs indexed over $i = 1, \ldots, N$, similarly to (1), the individual TOA from BS i is:

$$\rho_{\text{ref},i} = R_{\text{ref},i} + \delta_{\text{ref}} - \delta_i + \eta_{\text{ref},i}, \tag{2}$$

where the unknowns are δ_{ref} and δ_i. Choosing one BS as reference, and denoting it with subscript m, the ICCB between a BS i and the reference m is defined as $\delta_{i,m} = \delta_i - \delta_m$, which could be estimated based on (2) through single-difference, written as:

$$\begin{cases} \widehat{\delta}_{1,m} = (\rho_{\text{ref},1} - R_{\text{ref},1}) - (\rho_{\text{ref},m} - R_{\text{ref},m}) \\ \widehat{\delta}_{2,m} = (\rho_{\text{ref},2} - R_{\text{ref},2}) - (\rho_{\text{ref},m} - R_{\text{ref},m}) \\ \quad\vdots \\ \widehat{\delta}_{m,m} = (\rho_{\text{ref},m} - R_{\text{ref},m}) - (\rho_{\text{ref},m} - R_{\text{ref},m}) \\ \quad\vdots \\ \widehat{\delta}_{N,m} = (\rho_{\text{ref},N} - R_{\text{ref},N}) - (\rho_{\text{ref},m} - R_{\text{ref},m}) \end{cases}, \tag{3}$$

which describes the clock bias differences of different BSs. For better understanding, Fig. 2 shows the relation between ICCB and the clock bias of the UE and PRU.

C. ICCB SMOOTHING FOR NOISE MITIGATION

While (3) provides the raw ICCB, real-world TOA measurements from SSBs are inevitably corrupted by noise. In a static scenario, multipath reflections are largely time-invariant and introduce a systematic bias that cannot be reduced by temporal averaging. However, time-varying noise components, such as thermal noise and receiver clock jitter, cause the ICCB estimates to fluctuate over time. These fluctuations propagate directly into the ranging measurements, degrading their accuracy.

To mitigate this noise, we apply a moving average filter. Since the reference receiver is static, no motion dynamics need to be modeled. As shown in Section IV-B, the estimated ICCB exhibits rapid fluctuations dominated by measurement noise. The moving average filter is adopted as a model-free approach that suppresses this high-frequency noise without requiring an explicit clock drift model. While more sophisticated filtering techniques, such as a Kalman filter with a clock state model, could be investigated, they would require characterization of the specific oscillators used in the commercial BS equipment. The moving average provides an effective and practical solution for the static scenario considered here. We therefore filter the ICCB values using a moving average window of length T-second, expressed as:

$$\bar{\delta}_{i,m} = \frac{1}{T}\sum_{k=0}^{T-1} \widehat{\delta}_{i,m}(t-k), \tag{4}$$

where $\widehat{\delta}_{i,m}(t-k)$ represents the instantaneous ICCB measurement acquired by the reference receiver at time $t-k$, which constitutes the input to the moving average filter. Such a smoothed ICCB is used to align the clock bias between different cellular signals while suppressing the noise from the PRU. The choice of the window size T involves a trade-off between noise suppression and the ability to track potential ICCB drift. A sensitivity analysis over T is presented in Section IV-C to quantify this trade-off.

D. UE POSITIONING

By accounting for the ICCB $\delta_{i,m}$, we rewrite the UE ranging in (1) as:

$$\begin{aligned} \rho_{\text{UE},i} &= R_{\text{UE},i} + \delta_{\text{UE}} - (\delta_{i,m} + \delta_m) + \eta_{\text{UE},i} \\ &= R_{\text{UE},i} + \delta_{\text{rel}} - \delta_{i,m} + \eta_{\text{UE},i}\,, \end{aligned} \tag{5}$$

where $\delta_{i,m}$ is the ICCB compensation that can be measured with a PRU receiver. $\delta_{\text{rel}} = \delta_{\text{UE}} - \delta_m$ represents the relative clock bias between the UE and the reference BS. This implies that the PRU assists UE positioning with the compensation of the pairwise clock biases between BSs. This operation reduces the number of UE positioning unknowns from $(3+N)$ to $(3+1)$, at the cost of needing a PRU inside the cellular positioning architecture.

In practice, given the observed UE ranging measurement $\rho_{\text{UE},i}$, the corrected ranging measurement $\rho^{\text{corr}}_{\text{UE},i}$ using smoothed ICCB is:

$$\rho^{\text{corr}}_{\text{UE},i} = \rho_{\text{UE},i} + \bar{\delta}_{i,m}, \tag{6}$$

where $\bar{\delta}_{i,m}$ is the smoothed ICCB compensation calculated via (4), which becomes the instantaneous correction when $T = 1$ s. In practice, for each UE TOA measurement at time t, the ICCB correction at the same time epoch is applied. In the

smoothed case, $\bar{\delta}_{i,m}$ is computed by averaging the preceding T seconds of ICCB estimates; in the instantaneous case ($T = 1$ s), the single ICCB estimate at time t is used directly. To estimate the UE location, we define the unknown state vector as $\mathbf{x} = [\mathbf{p}_{\text{UE}}^{\top}\ \delta_{\text{rel}}]^{\top}$. The problem can be formulated as a non-linear least squares estimation:

$$\widehat{\mathbf{x}} = \arg\min_{\mathbf{x}} \left\| \boldsymbol{\rho}_{\text{UE}}^{\text{corr}} - \mathbf{h}(\mathbf{x}) \right\|_{\Omega}^{2}, \tag{7}$$

where $\boldsymbol{\rho}_{\text{UE}}^{\text{corr}} = [\rho_{\text{UE},1}^{\text{corr}} \cdots \rho_{\text{UE},N}^{\text{corr}}]^{\top}$ is the vector of corrected TOA measurements, and Ω represents the covariance matrix. The non-linear measurement model $\mathbf{h}(\mathbf{x})$ is defined as:

$$\mathbf{h}(\mathbf{x}) = \begin{bmatrix} \|\mathbf{p}_{\text{UE}} - \mathbf{p}_1\| + \delta_{\text{rel}} \\ \vdots \\ \|\mathbf{p}_{\text{UE}} - \mathbf{p}_N\| + \delta_{\text{rel}} \end{bmatrix}, \tag{8}$$

where $\mathbf{p}_i$ denotes the known coordinates of the i-th BS.

IV. EXPERIMENT AND RESULT

A. DATA OVERVIEW

Data acquisition was performed using two Rohde & Schwarz TSMA6 network scanners configured to passively receive 5G SSBs broadcasted by BSs. Such professional equipment has also been used in previous researches [1], [19], [38]. Field measurements were conducted in a rural area featuring open terrain in suburban outskirts. This rural open-terrain setting features reduced multipath complexity compared to urban or indoor environments, and it is used as a controlled baseline to isolate the effect of the ICCB on positioning accuracy. The two scanners were deployed at fixed positions, as shown in Fig. 3, with ground-truth coordinates measured using real-time kinematic (RTK) GNSS technology. The RTK GNSS receiver used for ground truth is the multi-constellation Swift Navigation Piksi Multi, which provides cm-level accuracy. This accuracy is marginal with respect to the 5G positioning results obtained in this work. One scanner is used as UE, and the other as PRU. The SSB TOAs were measured with respect to six BSs, two of them co-located, i.e., they refer to two transmission reception points (TRPs) of the same 5G site, mounted on the same pylon. The physical cell IDs (PCIs) uniquely identified the TRPs across the five sites. The BSs belong to the same mobile operator. The 5G network operates at 3.68 GHz and it is compliant with 3GPP Release 15 standard. The use of Release 15 SSB signals reflects the current state of commercial network deployments, where dedicated positioning signals introduced in Release 16 (e.g., PRSs) are not yet widely activated by operators. The proposed ICCB correction framework is signal-agnostic and directly applicable to higher-quality TOA measurements from PRS or SRS in Release 16 and beyond, where the reduced measurement noise would further enhance the correction effectiveness. The 5G SSB configuration follows the setup used in [1], [19], and [38], i.e., eight beams are transmitted according to SSB pattern C for numerology 1, with a periodicity of 20 ms. Each beam, if received, is associated with a per-beam TOA measured by the scanner. Such TOAs are adjusted by the transmit symbol time in the 5G slot as dictated by the transmit pattern. Signal metrics like TOA, synchronization signal reference signal received power (SS-RSRP), and signal-to-interference-plus-noise ratio (SINR) were logged for all detectable SSBs. Three independent measurement campaigns were conducted at the same rural location on different days, referred to as Test 1, Test 2, and Test 3, to assess the repeatability of the proposed approach. A qualitative illustration of the scenario is outlined in Fig. 3.

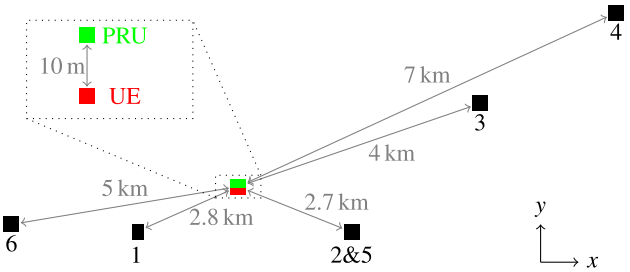

FIGURE 3. Geometrical settings of the positioning problem.

B. INTER-CELL CLOCK BIAS STABILITY

The ICCB characterization presented in this section is based on Test 1 as a representative example, since the qualitative behavior of the ICCB (stability, magnitude, and noise level) is consistent across the three campaigns.

Equations (3) and (5) show that the synchronization uncertainty measured at the PRU propagates to the UE TOA through the ICCB. To assess this, the stability of ICCB is analyzed using measurements from the reference receiver over a 10-minute window. As shown in Fig. 4, the single-difference clock bias $\delta_{i,m}$ between the reference m (PCI 3) and other BSs cellular signal exhibits stability yet with a large variance due to inherent measurement noise. This noise amplification effect is further quantified in Table 1, where the standard deviations (stds) for different PCIs range from 6.2 m to 32.6 m. A low standard deviation indicates stable ICCB estimates from consistent and reliable TOA measurements, while a high standard deviation reflects noisy TOA measurements that lead to fluctuating ICCB estimates. The variation across PCIs is attributed to differences in received signal quality and propagation conditions. For instance, PCIs 2 and 5, which are co-located and benefit from favorable propagation conditions, exhibit the lowest standard deviations (6.2 m and 7.1 m), while PCIs 1 and 6 show higher values (29.4 m and 32.6 m) due to lower received signal quality.

To mitigate these effects, the ICCBs are processed using a smoothing filter, with the results illustrated in Fig. 4b. Both the original and smoothed ICCB values are subsequently evaluated within the positioning solution. Finally, Fig. 5 compares the ICCB estimates calculated at the PRU and the UE (using ground-truth location for the latter). While ICCBs are theoretically independent of the receiver,

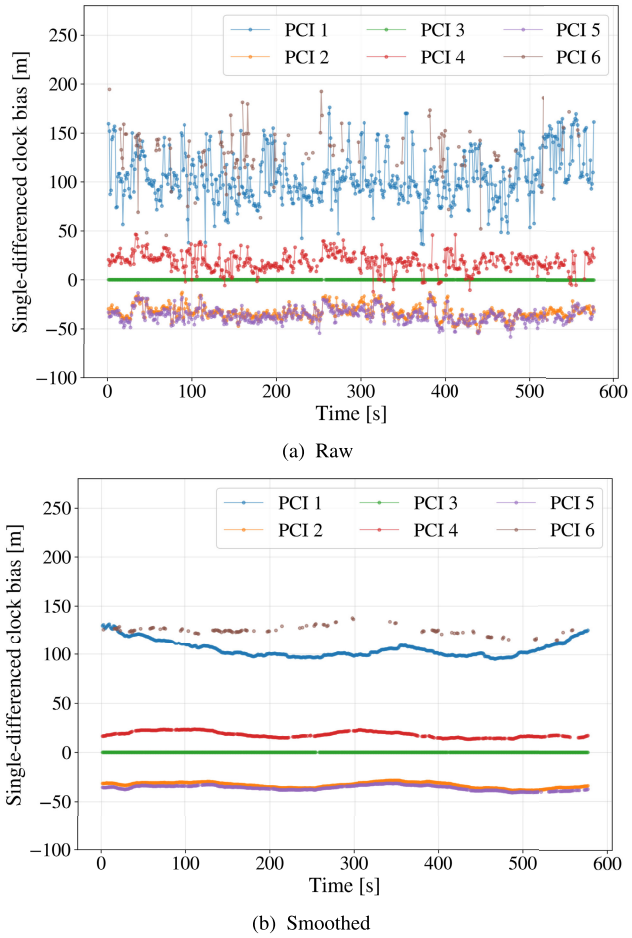

FIGURE 4. Estimated ICCB stability over time measured by the PRU with respect to five BSs and a reference BS. Raw and smoothed versions are shown. Values are converted into meter for an easier interpretability.

the results in Fig. 5 demonstrate that their respective estimates diverge in practice due to local measurement noise, confirming the propagation relationship defined in (5).

The 10 m UE–PRU separation adopted in our experiment reflects a deliberate design choice rather than a limitation of the correction itself. Since the ICCB is fundamentally a transmitter-side impairment originating from BS clock offsets, the PRU-derived correction is, in an ideal line-of-sight (LOS) scenario, theoretically valid over arbitrary UE–PRU separations. In practical deployments, the effective correctability is bounded by spatial decorrelation effects, angle-dependent antenna group delays, and different local scattering clusters. The 10 m setup ensures a quasi-isotropic local environment in line with the spatial consistency principles of 3GPP TR 38.901, so that the PRU and UE share nearly identical propagation conditions, allowing the validation of the systematic clock-bias correction with minimal confounding environmental effects.

C. POSITIONING ACCURACY

The considered ICCB compensation method is evaluated under four distinct positioning configurations: SD weighted least squares (WLS) utilizing smoothed ICCB corrections, where the weight for each BS measurement is derived from the physical broadcast channel (PBCH)-SINR as $w_i = \sqrt{10^{\mathrm{SINR}_{i,\mathrm{dB}}/10}}$, following the approach in [19]; SD ordinary least squares (OLS) incorporating the smoothed ICCB in (6); SD OLS with the instantaneous ICCB measurements in (6) when $T = 1$; DD OLS (reference PCI 3); and OLS without ICCB compensation.

TABLE 1. Mean and standard deviation (std.) of the ICCBs.

PCI	Mean [m]	std [m]
1	105.5	29.4
2	-33.3	6.2
3	0	0
4	18.4	10.1
5	-35.9	7.1
6	129.8	32.6

Concerning Test 1, Fig. 6 shows the positioning outcomes over space as well as their error ellipses, while Fig. 7 illustrates the positioning performance across different time epochs. Besides, Table 2 quantifies key statistical metrics across the three tests. These comparative analyses reveal several significant patterns.

Both SD and DD methods demonstrate substantial accuracy improvements over the uncompensated OLS solution, which exhibited the necessity of dealing with the inaccurate synchronization. Across the three tests, the mean error for uncompensated OLS ranges from 75.9 to 79.8 m, while the ICCB-enhanced methods achieve 12.7–29.5 m, confirming that ICCB compensation reduces errors by 73%–84%. The consistent performance across Tests 1 and 2 (both yielding a mean error of about 20 m for OLS with smoothed ICCB) demonstrates the repeatability of the proposed approach, while Test 3 shows even better performance (12.7 m mean error), likely due to more favorable channel conditions at the time of that experiment.

The SD solution can outperform the DD case because forming double differences, while effectively eliminating common clock errors, also amplifies the measurement noise. Such DD operation generates an accurate solution when the measurement noise is small, such as DD carrier phase [40]. However, the noise for SSB measurement could reach tens of meters [38]. By differencing observations, the uncorrelated noise from the reference BS is propagated into the final DD observation, increasing its overall noise level.

Remarkably, in Tests 1 and 2, the smoothed ICCB variants yield superior results to the instantaneous ICCB implementation: the mean error is reduced from 25.2 m to 20.6 m (Test 1) and from 24.9 m to 20.1 m (Test 2), corresponding to improvements of about 18%–19%. These gains underscore the value of the proposed smoothing algorithm.

To further investigate the effect of the smoothing window size, a sensitivity analysis is conducted on Test 1 over

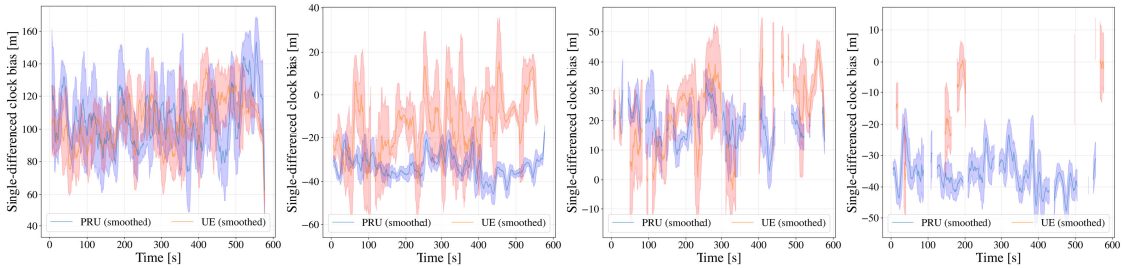

(a) PCI 1 (b) PCI 2 (c) PCI 4 (d) PCI 5

FIGURE 5. Mean and standard deviation of ICCB estimated at the UE and PRU. The time series is smoothed with a moving average filter (window size: 10 s) and converted into meter for easier interpretability. The truncation of some time series is due to intermittent signal availability, as the receivers may not detect SSB from all BSs at every time epoch.

$T = 1, 5, 10, 20, 30, 50$, and 100 s using the SD OLS configuration, with performances reported in Table 3. The selected $T = 100$ s is then applied to all three tests for the aggregated performance summarized by the cumulative density function (CDF) in Fig. 8. Increasing T consistently reduces the mean and root mean square error (RMSE) errors, with diminishing returns beyond $T = 30$ s. The 90th percentile error stabilizes around 40 m for $T \geq 10$ s. A longer averaging window provides greater noise suppression but may introduce lag when the ICCB drifts rapidly, as the smoothed correction would reflect a past state rather than the current one. In the considered static scenario, the ICCB mean is relatively stable over the 10-minute observation period, and the fluctuations are dominated by measurement noise, which favors a larger T. In this work, $T = 100$ s is adopted as it provides the best overall performance for the considered scenario. In deployments with faster clock drift, a shorter window or adaptive filtering may be necessary to balance noise suppression and tracking responsiveness.

The WLS approach with smoothed ICCB achieves performance comparable to OLS with smoothed ICCB, with a marginally higher mean error across all three tests (e.g., 21.0 m vs 20.6 m in Test 1, and 13.4 m vs 12.7 m in Test 3) and similar RMSE. In the considered static scenario, the signal-quality-based weighting does not yield significant improvement over OLS, as the dominant error source after ICCB compensation is multipath-induced TOA bias rather than thermal noise, and measurements with high SINR may still be affected by specular reflections. The comprehensive error distribution analysis in Fig. 8 reveals that 90% of positions using ICCB compensation achieve errors below 40 m, while uncompensated solutions exhibit a 90-th percentile error exceeding 80 m.

Finally, we note that the presented results are obtained in a static rural/open-sky-like environment and should not be directly extrapolated to more challenging propagation conditions. Scenarios such as urban canyons, industrial indoor environments, or non-line-of-sight (NLOS)-dominated settings exhibit stronger multipath and interference effects, which would introduce additional biases into the TOA measurements and potentially degrade the effectiveness of the PRU-derived ICCB correction. Validating the proposed framework in such environments represents an important direction for future work.

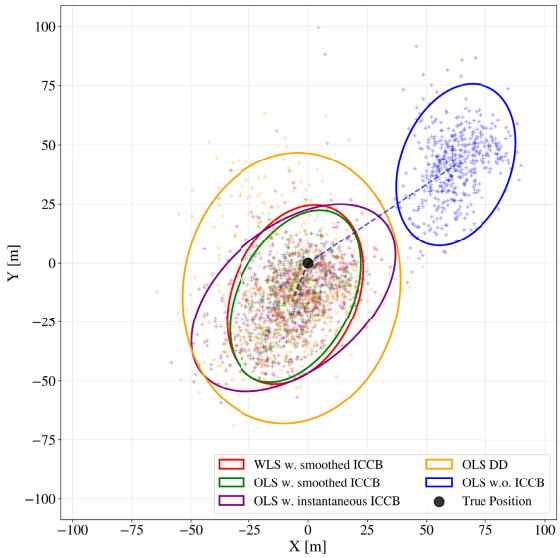

FIGURE 6. 5G positioning estimation for different algorithms with their error ellipses at 95% confidence. Axes are in meters relative to the ground-truth position.

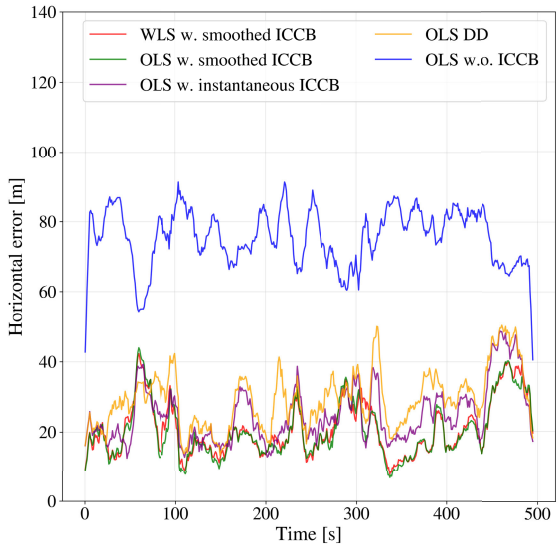

FIGURE 7. Time series of UE positioning error [m] for different algorithms. For a better visual clarity, the positioning error is plotted using a 10-seconds moving average.

TABLE 2. Static performance comparison across three independent tests conducted at the same rural location on different days. Values are in [m].

Test	Stat	WLS w. smoothed ICCB	OLS w. smoothed ICCB	OLS w. instantaneous ICCB	OLS DD	OLS w.o. ICCB
1	Mean	21.0	20.6	25.2	29.5	75.9
	RMSE	24.4	24.2	28.9	32.8	77.0
2	Mean	20.4	20.1	24.9	29.4	76.0
	RMSE	23.8	23.6	28.6	32.6	77.1
3	Mean	13.4	12.7	13.7	17.9	79.8
	RMSE	15.4	14.5	16.0	21.7	80.2

TABLE 3. Sensitivity analysis of the smoothing window size T. Positioning error values are in [m].

T [s]	Mean	RMSE	Max	90th pct.
1	25.68	30.01	111.96	46.38
5	23.38	27.07	132.86	41.71
10	22.44	25.98	103.45	40.31
20	21.88	25.54	119.04	40.68
30	21.45	24.91	71.48	40.59
50	21.06	24.53	66.43	40.75
100	20.48	24.01	99.61	39.01

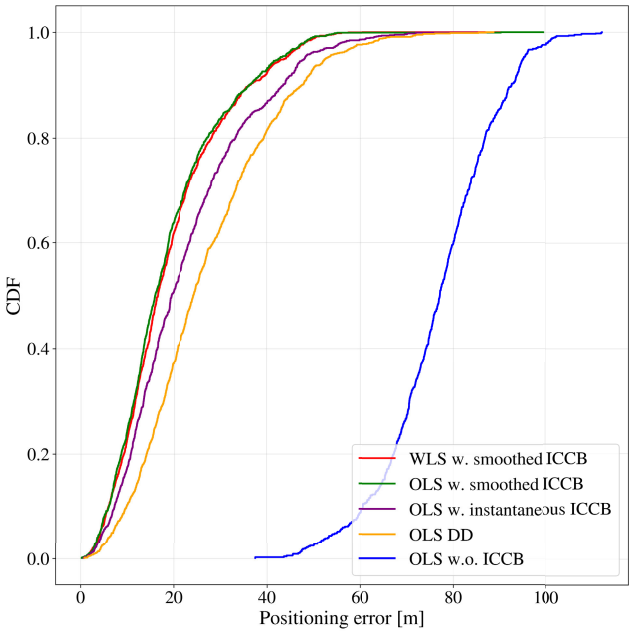

FIGURE 8. Cumulative density function of the UE positioning error [m] aggregated across Tests 1, 2, and 3 for different algorithms.

V. CONCLUSION AND FUTURE WORK

This paper introduced a method to enable standalone positioning with opportunistic 5G SSB measurements. By using a reference station to estimate the ICCB, the method mitigates the synchronization error affecting the TOA measurements at the UE. The experimental evaluation, based on three independent measurement campaigns conducted at the same rural location on different days and comparing four distinct implementations, shows that ICCB compensation provides a 73%–84% reduction in positioning errors compared to uncompensated solutions, with mean errors decreasing from 75.9–79.8 m to 12.7–25.2 m. Besides, the proposed smoothed ICCB provides about an 18%–19% accuracy improvement over instantaneous ICCB and DD implementations through effective noise suppression. The results confirm that the proposed ICCB compensation framework is highly effective, paving the way for the practical use of 5G in location-based services. The achieved mean error of approximately 20 m is best understood as a feasibility demonstration of moderate-accuracy positioning under the constraints of opportunistic SSB-TOA measurements and the limited effective bandwidth (7.2 MHz) of the current commercial Release 15 deployment at 3.68 GHz. Finer TOA precision, and consequently higher positioning accuracy, is expected with the adoption of Release 16 PRS (which supports larger bandwidths) and Release 18 features such as bandwidth aggregation and carrier phase positioning.

In the future, we intend to investigate hybrid positioning solutions fusing 5G TOA measurements with on-board sensors, such as inertial measurement units (IMUs) and GNSS, to provide a more resilient navigation suite for IIoT applications. The potential for multi-level fusion network structures and Bayesian approaches to dynamically adapt to non-linear error sources also represents a promising avenue for improving the accuracy. Besides, a study on the optimal deployment and density of PRUs within a commercial network is envisioned to understand the trade-off between system complexity and the achievable coverage of high-accuracy positioning services. Furthermore, investigating the spatial robustness of the PRU-derived correction by varying the UE–PRU separation across multiple locations is an important direction for future work.

LIST OF ACRONYMS

3GPP	3rd Generation Partnership Project.
5G	fifth generation.
BS	base station.
CBM	clock bias monitoring.
CDF	cumulative density function.
CPASS	carrier-phase positioning algorithm for systems without synchronization.
CPP	carrier phase positioning.
DD	double-difference.
GNSS	global navigation satellite systems.
gNB	gNodeB.
ICCB	inter-cell clock bias.
IIoT	industrial Internet of things.
IMU	inertial measurement unit.
LMF	location measurement function.
LOS	line-of-sight.
mmWave	millimeter wave.
NLOS	non-line-of-sight.
OLS	ordinary least squares.
PBCH	physical broadcast channel.
PCI	physical cell ID.

PRS	positioning reference signal.
PRU	positioning reference unit.
RMSE	root mean square error.
RTK	real-time kinematic.
SD	single-difference.
SDR	software-defined radio.
SINR	signal-to-interference-plus-noise ratio.
SRS	sounding reference signal.
SSB	synchronization signal block.
SS-RSRP	synchronization signal reference signal received power.
TOA	time of arrival.
TRP	transmission reception point.
UE	user equipment.
WLS	weighted least squares.

REFERENCES

[1] M. Brambilla, M. Alghisi, B. Camajori Tedeschini, A. Fumagalli, F. C. Grec, L. Italiano, C. Pileggi, L. Biagi, S. Bianchi, A. Gatti, A. Goia, M. Nicoli, and E. Realini, "Integration of 5G and GNSS technologies for enhanced positioning: An experimental study," *IEEE Open J. Commun. Soc.*, vol. 5, pp. 7197–7215, 2024.

[2] Q. Liu, C. Gao, A. Xhafa, W. Gao, J. A. López-Salcedo, and G. Seco-Granados, "Performance analysis of GNSS + 5G hybrid positioning algorithms for smartphones in urban environments," *IEEE Trans. Instrum. Meas.*, vol. 73, pp. 1–9, 2024.

[3] A. Gonzalez-Garrido, J. Querol, H. Wymeersch, and S. Chatzinotas, "Joint communication and navigation from LEO multi-beam satellite," *IEEE Open J. Commun. Soc.*, vol. 6, pp. 4384–4404, 2025.

[4] H. Alshaer, A. Ganau, D. Brilhante, C. Cleary, M. A. Ullah, and V. Kramar, "Next-generation integrated communications, navigation, and surveillance services," in *Proc. Integr. Commun., Navigat. Surveill. Conf. (ICNS)*, Apr. 2025, pp. 1–10.

[5] M. Abuyaghi, S. Si-Mohammed, G. Shaker, and C. Rosenberg, "Positioning in 5G networks: Emerging techniques, use cases, and challenges," *IEEE Internet Things J.*, vol. 12, no. 2, pp. 1408–1427, Jan. 2025.

[6] F. Mogyorósi, P. Revisnyei, A. Pašić, Z. Papp, I. Törös, P. Varga, and A. Pašić, "Positioning in 5G and 6G networks—A survey," *Sensors*, vol. 22, no. 13, p. 4757, Jun. 2022.

[7] G. Jornod and M. Stark, "Positioning evolutions in 5G standardization: Potential, solutions, and challenges of sidelink positioning for connected mobility," *IEEE Veh. Technol. Mag.*, vol. 20, no. 3, pp. 106–114, Sep. 2025.

[8] S. Dwivedi, R. Shreevastav, F. Munier, J. Nygren, I. Siomina, Y. Lyazidi, D. Shrestha, G. Lindmark, P. Ernström, E. Stare, S. M. Razavi, S. Muruganathan, G. Masini, Å. Busin, and F. Gunnarsson, "Positioning in 5G networks," *IEEE Commun. Mag.*, vol. 59, no. 11, pp. 38–44, Nov. 2021.

[9] W. Chen, J. Montojo, J. Lee, M. Shafi, and Y. Kim, "The standardization of 5G-advanced in 3GPP," *IEEE Commun. Mag.*, vol. 60, no. 11, pp. 98–104, Nov. 2022.

[10] S. Bartoletti and N. B. Melazzi, *Positioning Location-based Analytics 5G and Beyond*. Hoboken, NJ, USA: Wiley, 2023.

[11] L. Italiano, B. Camajori Tedeschini, M. Brambilla, H. Huang, M. Nicoli, and H. Wymeersch, "A tutorial on 5G positioning," *IEEE Commun. Surveys Tuts.*, vol. 27, no. 3, pp. 1488–1535, Jun. 2025.

[12] A. Saikko, J. Talvitie, J. Säe, J. Pirskanen, and M. Valkama, "Positioning and tracking in DECT-2020 NR with proactive anchor selection for range, angle, and RSS measurements," *IEEE J. Indoor Seamless Positioning Navigat.*, vol. 3, pp. 70–80, 2025.

[13] F. Morselli, S. Modarres Razavi, M. Z. Win, and A. Conti, "Soft information-based localization for 5G networks and beyond," *IEEE Trans. Wireless Commun.*, vol. 22, no. 12, pp. 9923–9938, Dec. 2023.

[14] K. Witrisal, P. Meissner, E. Leitinger, Y. Shen, C. Gustafson, F. Tufvesson, K. Haneda, D. Dardari, A. F. Molisch, A. Conti, and M. Z. Win, "High-accuracy localization for assisted living: 5G systems will turn multipath channels from foe to friend," *IEEE Signal Process. Mag.*, vol. 33, no. 2, pp. 59–70, Mar. 2016.

[15] J. Talvitie, T. Levanen, M. Koivisto, T. Ihalainen, K. Pajukoski, and M. Valkama, "Positioning and location-aware communications for modern railways with 5G new radio," *IEEE Commun. Mag.*, vol. 57, no. 9, pp. 24–30, Sep. 2019.

[16] X. Jia, P. Liu, W. Qi, S. Liu, Y. Huang, W. Zheng, M. Pan, and X. You, "Link-level simulator for 5G localization," *IEEE Trans. Wireless Commun.*, vol. 22, no. 8, pp. 5198–5213, Aug. 2023.

[17] Z. Abu-Shaban, X. Zhou, T. Abhayapala, G. Seco-Granados, and H. Wymeersch, "Error bounds for uplink and downlink 3D localization in 5G millimeter wave systems," *IEEE Trans. Wireless Commun.*, vol. 17, no. 8, pp. 4939–4954, Aug. 2018.

[18] W. Dong, L. Chen, Z. Ju, T. Zhou, Z. Liu, and R. Chen, "Beam-switching-based time-of-arrival ranging on commercial 5G NR signals for outdoor positioning," *IEEE Trans. Wireless Commun.*, vol. 25, pp. 3121–3136, 2026.

[19] B. Camajori Tedeschini, M. Brambilla, L. Italiano, S. Reggiani, D. Vaccarono, M. Alghisi, L. Benvenuto, A. Goia, E. Realini, F. Grec, and M. Nicoli, "A feasibility study of 5G positioning with current cellular network deployment," *Sci. Rep.*, vol. 13, no. 1, p. 15281, Sep. 2023.

[20] M. Neinavaie, J. Khalife, and Z. M. Kassas, "Cognitive opportunistic navigation in private networks with 5G signals and beyond," *IEEE J. Sel. Topics Signal Process.*, vol. 16, no. 1, pp. 129–143, Jan. 2022.

[21] K. Shamaei and Z. M. Kassas, "Receiver design and time of arrival estimation for opportunistic localization with 5G signals," *IEEE Trans. Wireless Commun.*, vol. 20, no. 7, pp. 4716–4731, Jul. 2021.

[22] W. Dong, L. Chen, Z. Ju, Z. Jiao, and R. Chen, "Time-of-arrival estimation in challenging environments using commercial 5G NR signals for outdoor positioning," *IEEE Internet Things J.*, vol. 12, no. 12, pp. 20722–20735, Jun. 2025.

[23] X. Zhou, L. Chen, and Y. Ruan, "Indoor positioning with multibeam CSI from a single 5G base station," *IEEE Sensors Lett.*, vol. 8, no. 1, pp. 1–4, Jan. 2024.

[24] A. Abdallah, J. Khalife, and Z. M. Kassas, "Exploiting on-demand 5G downlink signals for opportunistic navigation," *IEEE Signal Process. Lett.*, vol. 30, pp. 389–393, 2023.

[25] S. Shahcheraghi and Z. M. Kassas, "Carrier-to-noise ratio improvement of 5G signals via beamforming for TOA-based opportunistic navigation," in *Proc. IEEE Wireless Commun. Netw. Conf. (WCNC)*, Mar. 2025, pp. 1–6.

[26] P. Dinh, Y. Feng, E. Baena, Y. Han, W. Qi, Z. Xu, M. Ghoshal, P. Closas, D. Koutsonikolas, and J. Widmer, "mm-NOLOC: mmWave-based localization for mobile networks without 3GPP location service," in *Proc. 26th Int. Symp. Theory, Algorithmic Found., Protocol Design Mobile Netw. Mobile Comput.*, Oct. 2025, pp. 21–30.

[27] L. Petrucci, S. Zanini, I. Palamà, N. B. Melazzi, and S. Bartoletti, "Localization in 5G and beyond: A multi-objective approach for accuracy, latency, and resilience," *IEEE Trans. Mobile Comput.*, vol. 24, no. 12, pp. 12771–12783, Dec. 2025.

[28] I. Palamà, Y. Lizarribar, L. M. Monteforte, G. Santaromita, S. Bartoletti, D. Giustiniano, G. Bianchi, and N. B. Melazzi, "5G positioning with software-defined radios," *Comput. Netw.*, vol. 250, Aug. 2024, Art. no. 110595. [Online]. Available: https://www.sciencedirect.com/science/article/pii/S1389128624004274

[29] I. Palamà, S. Bartoletti, G. Bianchi, and N. Bléfari-Melazzi, "Experimental assessment of SDR-based 5G positioning: Methodologies and insights," *Ann. Telecommun.*, vol. 79, nos. 5–6, pp. 301–313, 2023.

[30] L. Chen, X. Zhou, F. Chen, L.-L. Yang, and R. Chen, "Carrier phase ranging for indoor positioning with 5G NR signals," *IEEE Internet Things J.*, vol. 9, no. 13, pp. 10908–10919, Jul. 2022.

[31] Z. Liu, L. Chen, X. Zhou, Z. Jiao, G. Guo, and R. Chen, "Machine learning for time-of-arrival estimation with 5G signals in indoor positioning," *IEEE Internet Things J.*, vol. 10, no. 11, pp. 9782–9795, Jun. 2023.

[32] P. Morri, V. Bernazzoli, M. Brambilla, E. Moro, I. Filippini, and M. Nicoli, "An experimental assessment of 5G uplink ranging," in *Proc. IEEE Int. Workshop Metrol. Ind. 4.0 IoT (MetroInd4.0 IoT)*, May 2024, pp. 59–64.

[33] Y. Ruan, L. Chen, X. Zhou, Z. Liu, X. Liu, G. Guo, and R. Chen, "IPos-5G: Indoor positioning via commercial 5G NR CSI," *IEEE Internet Things J.*, vol. 10, no. 10, pp. 8718–8733, May 2023.

[34] J. A. d. Peral-Rosado, A. Y. Yildirim, A. P. Soderini, R. Mundlamuri, F. Kaltenberger, E. Rastorgueva-Foi, J. Talvitie, I. Lapin, and D. Flachs, "Initial experimentation of a real-time 5G mmWave downlink positioning testbed," *Eng. Proc.*, vol. 88, no. 1, p. 61, 2025. [Online]. Available: https://www.mdpi.com/2673-4591/88/1/61

[35] M. Moreno, D. Oxman, J. Sandoval, C. A. Azurdia-Meza, M. G. Gaitán, P. P. Játiva, and A. D. Firoozabadi, "NB-IoT path loss experimental measurements in urban outdoor environments," in *Proc. 14th Int. Symp. Commun. Syst.*, 2024, pp. 120–124.
[36] X. Cui, T. A. Gulliver, J. Li, and H. Zhang, "Vehicle positioning using 5G millimeter-wave systems," *IEEE Access*, vol. 4, pp. 6964–6973, 2016.
[37] A. Shastri, N. Valecha, E. Bashirov, H. Tataria, M. Lentmaier, F. Tufvesson, M. Rossi, and P. Casari, "A review of millimeter wave device-based localization and device-free sensing technologies and applications," *IEEE Commun. Surveys Tuts.*, vol. 24, no. 3, pp. 1708–1749, 3rd Quart., 2022.
[38] L. Barbieri, M. Brambilla, A. Goia, M. Nicoli, and A. Capone, "An experimental analysis on the readiness of currently deployed 5G networks for positioning," *IEEE Trans. Instrum. Meas.*, vol. 74, pp. 1–4, 2025.
[39] S. Fan, W. Ni, H. Tian, Z. Huang, and R. Zeng, "Carrier phase-based synchronization and high-accuracy positioning in 5G new radio cellular networks," *IEEE Trans. Commun.*, vol. 70, no. 1, pp. 564–577, Jan. 2022.
[40] A. Fouda, R. Keating, and H.-S. Cha, "Toward cm-level accuracy: Carrier phase positioning for IIoT in 5G-advanced NR networks," in *Proc. IEEE 33rd Annu. Int. Symp. Pers., Indoor Mobile Radio Commun. (PIMRC)*, Sep. 2022, pp. 782–787.
[41] *NG Radio Access Network (NG-RAN); Stage 2 Functional Specification of User Equipment (UE) Positioning in NG-RAN*, Standard (TS) 38.305, v18.6.0, 3rd Generation Partnership Project (3GPP), 2025.
[42] H.-S. Cha, G. Lee, A. Ghosh, M. Baker, S. Kelley, and J. Hofmann, "5G NR positioning enhancements in 3GPP release-I8," *IEEE Commun. Standards Mag.*, vol. 9, no. 1, pp. 22–27, Mar. 2025.
[43] X. Zhang, T. Wang, Z. Yao, and M. Lu, "Centimeter-level carrier phase positioning for ground-based positioning system without synchronization," *IEEE Trans. Veh. Technol.*, vol. 73, no. 10, pp. 15345–15358, Oct. 2024.
[44] T. Wang, Z. Yao, and M. Lu, "Cooperative carrier phase positioning for asynchronous narrowband positioning systems," *IEEE Trans. Veh. Technol.*, vol. 70, no. 10, pp. 10347–10358, Oct. 2021.
[45] *NG Radio Access Network (NG-RAN); Stage 2 Functional Specification of User Equipment (UE) Positioning in NG-RAN*, Standard (TS) 38.305, v17.8.0, 3rd Generation Partnership Project (3GPP), 2025.

PENGHUI XU (Member, IEEE) received the B.S. degree from South China Agricultural University, in 2015, and the M.Sc. degree in mechanical engineering and the Ph.D. degree from The Hong Kong Polytechnic University, in 2017 and 2025, respectively. During his doctoral studies, he was a Visiting Researcher with the Polytechnic University of Milan. After his master's degree, he mainly worked in machine learning algorithm development. He is currently a Postdoctoral Fellow with The Hong Kong Polytechnic University. His research interests include machine learning, GNSS urban localization, and multi-sensor integration for positioning.

MATTIA BRAMBILLA (Senior Member, IEEE) received the B.Sc. and M.Sc. degrees in telecommunication engineering and the Ph.D. degree (cum laude) in information technology from the Politecnico di Milano, Milan, Italy, in 2015, 2017, and 2021, respectively.

In 2019, he was a Visiting Researcher with the NATO Centre for Maritime Research and Experimentation, La Spezia, Italy. In 2021, he joined the Faculty of Dipartimento di Elettronica, Informazione e Bioingegneria (DEIB), Politecnico di Milano, as a Research Fellow. His research interests include signal processing, statistical learning, and data fusion for cooperative localization and communications.

Dr. Brambilla was a recipient of the 2024 Best Paper Award of Elsevier Vehicular Communications and the Best Student Paper Award at the 2018 IEEE Statistical Signal Processing Workshop. He is an Associate Editor of IEEE Open Journal of Signal Processing and ISIF *Journal of Advances in Information Fusion*.

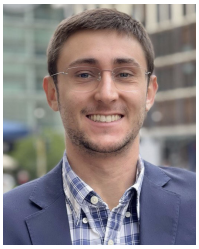

BERNARDO CAMAJORI TEDESCHINI (Member, IEEE) received the B.Sc. degree in computer science, the M.Sc. degree in telecommunication engineering, and the Ph.D. degree in information technology from the Politecnico di Milano, Milan, Italy, in 2019, 2021, and 2024, respectively.

In 2021, he was a Visiting Research Scientist with CERN, Geneva, Switzerland, where he worked on the CAFEIN Project, focusing on the development and deployment of a federated network platform. In 2024, he was a Visiting Ph.D. Student with the Wireless Information and Network Sciences Laboratory, Massachusetts Institute of Technology (MIT), Cambridge, MA, USA. His research interests encompass federated learning, machine learning for signal processing and sensing over networks, and localization methods.

Dr. Camajori Tedeschini was a recipient of the Dimitris N. Chorafas Foundation Prize, in 2025, and the Florian Daniel Award and the Roberto Rocca Doctoral Fellowship by MIT and the Politecnico di Milano.

MONICA NICOLI (Senior Member, IEEE) received the M.Sc. (Hons.) and Ph.D. degrees in communication engineering from the Politecnico di Milano, Milan, Italy, in 1998 and 2002, respectively.

She was a Visiting Researcher with ENI Agip, from 1998 to 1999, and with Uppsala University, in 2001. In 2002, she joined the Politecnico di Milano as a Faculty Member, where she is currently an Associate Professor in telecommunications with the Department of Management, Economics and Industrial Engineering. Her research interests include signal processing, machine learning, and wireless communications, with emphasis on smart mobility and the Internet of Things applications.

Dr. Nicoli was a recipient of the Marisa Bellisario Award, in 1999. She was a co-recipient of the Best Paper Awards of the IEEE Symposium on Joint Communications and Sensing, in 2021, the IEEE Statistical Signal Processing Workshop, in 2018, the IET Intelligent Transport Systems journal, in 2014, and the 2024 Best Paper Award of Elsevier Vehicular Communications. She served as an Associate Editor for IEEE Transactions on Intelligent Transportation Systems.